Composites Part B 80 (2015) 186–197

Contents lists available at ScienceDirect

Composites Part B

journal homepage: www.elsevier.com/locate/compositesb

Thermal uncertainty quantification in frequency responses of laminated composite plates

S. Dey [a, *], T. Mukhopadhyay [a], S.K. Sahu [b], G. Li [c], H. Rabitz [c], S. Adhikari [a]

[a] College of Engineering, Swansea University, UK
[b] Department of Civil Engineering, National Institute of Technology Rourkela, India
[c] Department of Chemistry, Princeton University, USA

ARTICLE INFO

Article history:
Received 27 January 2015
Received in revised form
27 April 2015
Accepted 1 June 2015
Available online 10 June 2015

Keywords:
A. Laminates
B. Vibration
C. Computational modelling
C. Statistical properties/methods
Thermal uncertainty

ABSTRACT

The propagation of thermal uncertainty in composite structures has significant computational challenges. This paper presents the thermal, ply-level and material uncertainty propagation in frequency responses of laminated composite plates by employing surrogate model which is capable of dealing with both correlated and uncorrelated input parameters. The present approach introduces the generalized high dimensional model representation (GHDMR) wherein diffeomorphic modulation under observable response preserving homotopy (D-MORPH) regression is utilized to ensure the hierarchical orthogonality of high dimensional model representation component functions. The stochastic range of thermal field includes elevated temperatures up to 375 K and sub-zero temperatures up to cryogenic range of 125 K. Statistical analysis of the first three natural frequencies is presented to illustrate the results and its performance.

1. Introduction

Composite materials are being increasingly utilized in aerospace applications due to high strength, stiffness, light weight and tailorable properties. They may be exposed to variation in environmental (hot or cold) conditions during the service life such as aircraft wing made of composite materials experiences a wide range of temperature variation from take-off to level-flight depending on altitude of flight. The stochasticity in frequency responses due to thermal effects on composites is an important criterion for overall design. In specific applications, the thermal effect acts as a fundamental factor for design consideration. These changes of thermal environments produce uncertain responses in the laminated composite structures. Hence the thermal condition has significant effect on the frequency characteristics and performance of composites. The natural frequency of composite structure under different thermo-mechanical loading conditions relies on its system parameters. The uncertainties of input parameters such as temperature, ply orientation angle and material properties lead to the uncertainties in the natural frequency of the composite structures. The stochasticity in the system's input parameters are considered in the analysis (for both individual and combined variation of inputs) so that the anticipated response can be turned out to be safe for the structure. Such engineering problems need to efficiently establish the correlation between high dimensional input parameters and interested output quantities. These structures can be characterized by probabilistic model using the small set of input data obtained from laboratory/field test or numerical simulation.

The free vibration of laminated plates with effect of environment has been considered earlier by Whitney and Ashton [1]. The effect of environments on the material properties of composites was studied by many researchers, for example, Strife and Prewo [2] and Bowles and Tompkins [3] and Seng et al. [4]. Ample published work is found on deterministic buckling analysis in conjunction to thermal and hygrothermal behavior [5–12]. The concept of random vibration is exhaustively utilised in many engineering application [13–15]. Most of the literature are deterministic in nature, which lacks in portraying the probable deviation caused by random input parameters. Due to presence of large number of inter-dependent factors in production of composites, the system input parameters are generally random in nature. The allowable responses for conventional material is expected to be close to their mean values as fewer parameters are involved in their production process while in contrast for composites, a range of random fluctuation in system

* Corresponding author.
E-mail addresses: infosudip@gmail.com, S.Dey@swansea.ac.uk (S. Dey).

http://dx.doi.org/10.1016/j.compositesb.2015.06.006
1359-8368/

parameter may occur due to large number of system properties. Even after ensuring the effective quality control of production process in sensitive applications, the allowable responses are normally found to scatter widely with respect to the mean values. The knowledge of input variabilities and corresponding range of stochastic responses may serve to control the purposes of lightweight design, which is one of the important characteristics for composites. Therefore the efficient computational modelling and analysis is needed considering randomness in material properties and ply orientation angle including the effect of thermal uncertainty to ensure optimization, operational safety and reliability. Such issues can be addressed by employing probabilistic method, which quantifies the uncertainties in frequency responses.

The novelty of the present study includes the stochastic analysis of natural frequencies for laminated composite plates subjected to uncertain thermo-mechanical loading. A surrogate model is employed by using the generalized high dimensional model representation (GHDMR) approach wherein D-MORPH (Diffeomorphic Modulation under Observable Response Preserving Homotopy) regression is employed to ensure the hierarchical orthogonality of HDMR component functions [16]. Random sampling high dimensional model representation (RS-HDMR) was employed for uncertainty quantification of natural frequency in composite plates considering three input parameters namely fibre-orientation angle, elastic modulus and mass density [17], wherein the input parameters are independent to each other. In contrast, investigation is also carried out with a new element for laminated composite plates [18] while stochastic modeling of unidirectional composites is studied considering delamination [19]. In the present study, the sources of uncertainty for natural frequency are considered as layer wise variation of material properties, ply orientation angle and temperature. Material properties of fibre reinforced composites are temperature dependent. Due to this reason, the input parameters become co-related to each other in case of layer wise combined variation of material properties, ply orientation angle and temperature. The co-related input parameters cannot be mapped for the corresponding output response using conventional high dimensional model representation (HDMR) approach different variants of HDMR can be found in available literature such as Cut-HDMR [20], RS-HDMR [21], mp-Cut-HDMR [22], Multicut-HDMR [23], lp-RS-HDMR [24] depending primarily on sampling scheme [16]. The present GHDMR can efficiently take care of both independent as well as co-related input parameters under a relaxed vanishing condition. The extended bases are used as basis functions to approximated HDMR component functions and D-MORPH regression is used to determine the coefficients in the GHDMR algorithm. The application of GHDMR is the first attempt of its kind in realm of laminated composites to take into account the effect of both non-correlated and/or correlated input parameters. In the present study, a random variable approach is employed in conjunction to finite element formulation to figure out the random eigenvalue problem. The numerical results are shown for first three natural frequencies with individual and combined layerwise variation of the stochastic input parameters. The present probabilistic approach is validated with Monte Carlo simulation wherein a small random variation is considered as tolerance zone.

2. Governing equations

Consider a laminated composite cantilever plate as furnished in Fig. 1(a,b) with thickness 't' consisting of n number of thin lamina, the stress strain relations in the presence of temperature can be represented as [25].

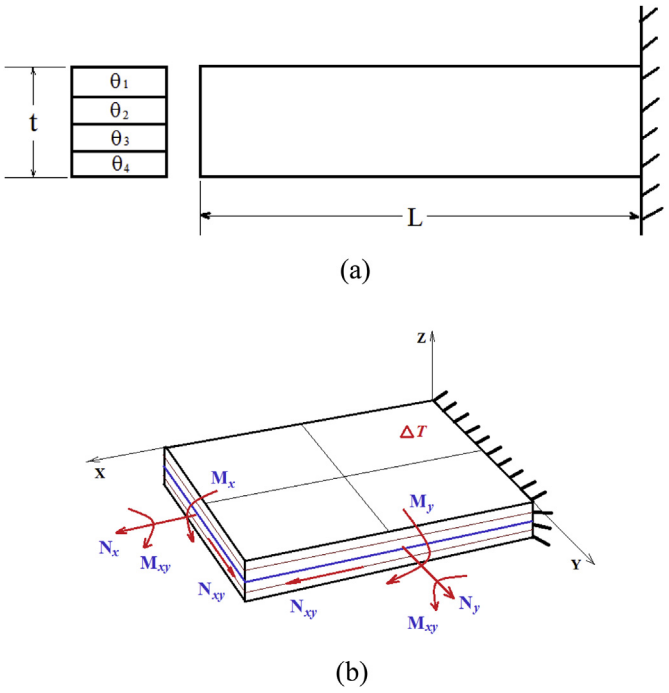

Fig. 1. (a) Laminated composite cantilever plate. (b) Force and moment resultants diagram.

$$\begin{Bmatrix} \sigma_x(\tilde{\omega}) \\ \sigma_y(\tilde{\omega}) \\ \tau_{xy}(\tilde{\omega}) \end{Bmatrix} = \begin{bmatrix} \overline{Q}_{11}(\tilde{\omega}) & \overline{Q}_{12}(\tilde{\omega}) & \overline{Q}_{16}(\tilde{\omega}) \\ \overline{Q}_{12}(\tilde{\omega}) & \overline{Q}_{22}(\tilde{\omega}) & \overline{Q}_{26}(\tilde{\omega}) \\ \overline{Q}_{16}(\tilde{\omega}) & \overline{Q}_{26}(\tilde{\omega}) & \overline{Q}_{66}(\tilde{\omega}) \end{bmatrix} \begin{Bmatrix} \varepsilon_x^o - e_x^T(\tilde{\omega}) \\ \varepsilon_y^o - e_y^T(\tilde{\omega}) \\ \gamma_{xy}^o - e_{xy}^T(\tilde{\omega}) \end{Bmatrix} \tag{1}$$

and

$$\begin{Bmatrix} \tau_{xz}(\tilde{\omega}) \\ \tau_{yz}(\tilde{\omega}) \end{Bmatrix} = \begin{bmatrix} \overline{Q}_{44}(\tilde{\omega}) & \overline{Q}_{45}(\tilde{\omega}) \\ \overline{Q}_{45}(\tilde{\omega}) & \overline{Q}_{55}(\tilde{\omega}) \end{bmatrix} \begin{Bmatrix} \gamma_{xz}^o \\ \gamma_{yz}^o \end{Bmatrix} \tag{2}$$

where, σ_x, σ_y, τ_{xy},τ_{xz}, τ_{yz} are normal and shear stresses; ε_x^o, ε_y^o, γ_{xy}^o γ_{xz}^o, γ_{yz}^o are normal and shear strains. The e_x^T, e_y^T, e_{xy}^T values are the thermal strain components due to temperature in x–y reference axes, which are derived from the corresponding values in the fiber axes after applying the transformations expressed as

$$\begin{aligned} \left\{e^T(\tilde{\omega})\right\} &= \begin{Bmatrix} e_x^T(\tilde{\omega}) \\ e_y^T(\tilde{\omega}) \\ e_{xy}^T(\tilde{\omega}) \end{Bmatrix} \\ &= \begin{bmatrix} Cos^2\theta(\tilde{\omega}) & Sin^2\theta(\tilde{\omega}) \\ Sin^2\theta(\tilde{\omega}) & Cos^2\theta(\tilde{\omega}) \\ -2Cos\theta(\tilde{\omega})Sin\theta(\tilde{\omega}) & 2Sin\theta(\tilde{\omega})Cos\theta(\tilde{\omega}) \end{bmatrix} \begin{Bmatrix} \alpha_1 \\ \alpha_2 \end{Bmatrix} \Delta T(\tilde{\omega}) \end{aligned} \tag{3}$$

where, $(\tilde{\omega})$ indicates the randomness of the corresponding variables and α_1, α_2 are the thermal expansion coefficients of lamina in longitudinal and lateral directions and their values are considered as -0.3×10^6 /K and 28.1×10^6 /K, respectively. $\Delta T(\tilde{\omega}) = T(\tilde{\omega}) - T_o(\tilde{\omega})$, where $T_o(\tilde{\omega})$ is the reference variable temperature in Kelvin. T is exposed random temperature in Kelvin. Here, $\theta(\tilde{\omega})$ denotes the random ply orientation angle of the lamina with reference to x-axis. The non-mechanical in-plane stress and moment resultants due to thermal environment are expressed as

$$\begin{Bmatrix} N_x^t(\tilde{\omega}) \\ N_y^t(\tilde{\omega}) \\ N_{xy}^t(\tilde{\omega}) \end{Bmatrix} = \sum_{k=1}^{n} \int_{Z_{k-1}}^{Z_k} \left[\overline{Q}_{ij}(\tilde{\omega})\right]_k \left[e^T(\tilde{\omega})\right]_k dz \quad \text{where } i,j = 1,2,6 \tag{4}$$

$$\text{and} \begin{Bmatrix} M_x^t(\tilde{\omega}) \\ M_y^t(\tilde{\omega}) \\ M_{xy}^t(\tilde{\omega}) \end{Bmatrix} = \sum_{k=1}^{n} \int_{Z_{k-1}}^{Z_k} \left[\overline{Q}_{ij}(\tilde{\omega})\right]_k \left[e^T(\tilde{\omega})\right]_k z dz \tag{5}$$

where $i,j = 1,2,6$

The force and moment resultants are modified to include the thermal field by the constitutive equations [26,27] for the composite plate are given by

$$\{F(\tilde{\omega})\} = [D(\tilde{\omega})]\{\varepsilon\} - \{F^t(\tilde{\omega})\} \tag{6}$$

where

$$\{F(\tilde{\omega})\} = \begin{bmatrix} N_x(\tilde{\omega}) & N_y(\tilde{\omega}) & N_{xy}(\tilde{\omega}) & M_x(\tilde{\omega}) & M_y(\tilde{\omega}) & M_{xy}(\tilde{\omega}) & Q_x(\tilde{\omega}) & Q_y(\tilde{\omega}) \end{bmatrix}^T \tag{7}$$

$$[D(\tilde{\omega})] = \begin{bmatrix} A_{11}(\tilde{\omega}) & A_{12}(\tilde{\omega}) & A_{16}(\tilde{\omega}) & B_{11}(\tilde{\omega}) & B_{12}(\tilde{\omega}) & B_{16}(\tilde{\omega}) & 0 & 0 \\ A_{12}(\tilde{\omega}) & A_{22}(\tilde{\omega}) & A_{26}(\tilde{\omega}) & B_{12}(\tilde{\omega}) & B_{22}(\tilde{\omega}) & B_{26}(\tilde{\omega}) & 0 & 0 \\ A_{16}(\tilde{\omega}) & A_{26}(\tilde{\omega}) & A_{66}(\tilde{\omega}) & B_{16}(\tilde{\omega}) & B_{26}(\tilde{\omega}) & B_{66}(\tilde{\omega}) & 0 & 0 \\ B_{11}(\tilde{\omega}) & B_{12}(\tilde{\omega}) & B_{16}(\tilde{\omega}) & D_{11}(\tilde{\omega}) & D_{12}(\tilde{\omega}) & D_{16}(\tilde{\omega}) & 0 & 0 \\ B_{12}(\tilde{\omega}) & B_{22}(\tilde{\omega}) & B_{26}(\tilde{\omega}) & D_{12}(\tilde{\omega}) & D_{22}(\tilde{\omega}) & D_{26}(\tilde{\omega}) & 0 & 0 \\ B_{16}(\tilde{\omega}) & B_{26}(\tilde{\omega}) & B_{66}(\tilde{\omega}) & D_{16}(\tilde{\omega}) & D_{26}(\tilde{\omega}) & D_{66}(\tilde{\omega}) & 0 & 0 \\ 0 & 0 & 0 & 0 & 0 & 0 & S_{44}(\tilde{\omega}) & S_{45}(\tilde{\omega}) \\ 0 & 0 & 0 & 0 & 0 & 0 & S_{45}(\tilde{\omega}) & S_{55}(\tilde{\omega}) \end{bmatrix} \tag{8}$$

The non-mechanical loads due to uncertain thermal condition

$$\{F^t(\tilde{\omega})\} = \begin{bmatrix} N_x^t(\tilde{\omega}) & N_y^t(\tilde{\omega}) & N_{xy}^t(\tilde{\omega}) & M_x^t(\tilde{\omega}) & M_y^t(\tilde{\omega}) & M_{xy}^t(\tilde{\omega}) & 0 & 0 \end{bmatrix}^T \tag{9}$$

$$\{\varepsilon\} = \begin{bmatrix} \varepsilon_x^o & \varepsilon_y^o & \gamma_{xy}^o & k_x & k_y & k_{xy} & \gamma_{xz}^o & \gamma_{yz}^o \end{bmatrix}^T \tag{10}$$

The stiffness coefficients are defined as [28].

$$\begin{bmatrix} A_{ij}(\tilde{\omega}), & B_{ij}(\tilde{\omega}), & D_{ij}(\tilde{\omega}) \end{bmatrix} = \sum_{k=1}^{n} \int_{Z_{k-1}}^{Z_k} \left[\overline{Q}_{ij}(\tilde{\omega})\right]_k \begin{bmatrix} 1, & z, & z^2 \end{bmatrix} dz$$

where $i,j = 1,2,6$ (11)

$$\text{and } [S_{ij}(\tilde{\omega})] = \alpha_{scf} \sum_{k=1}^{n} \int_{Z_{k-1}}^{Z_k} \left[\overline{Q}_{ij}(\tilde{\omega})\right]_k dz \quad \text{where } i,j = 4,5 \tag{12}$$

where α_{scf} is the shear correction factor and is assumed as 5/6. $[\overline{Q}_{ij}(\tilde{\omega})]$ in above Equations (11) and (12) is defined as

$$\left[\overline{Q}_{ij}(\tilde{\omega})\right] = [T_1(\tilde{\omega})]^{-1}[Q_{ij}(\tilde{\omega})][T_1(\tilde{\omega})]^{-T} \quad \text{for } i,j = 1,2,6 \tag{13}$$

$$\left[\overline{Q}_{ij}(\tilde{\omega})\right] = [T_2(\tilde{\omega})]^{-1}[Q_{ij}(\tilde{\omega})][T_2(\tilde{\omega})]^{-T} \quad \text{for } i,j = 4,5 \tag{14}$$

where

$$\left[T_1(\tilde{\omega})\right] = \begin{bmatrix} Cos^2\theta(\tilde{\omega}) & Sin^2\theta(\tilde{\omega}) & 2Sin\theta(\tilde{\omega})Cos\theta(\tilde{\omega}) \\ Sin^2\theta(\tilde{\omega}) & Cos^2\theta(\tilde{\omega}) & -2Cos\theta(\tilde{\omega})Sin\theta(\tilde{\omega}) \\ -Cos\theta(\tilde{\omega})Sin\theta(\tilde{\omega}) & Sin\theta(\tilde{\omega})Cos\theta(\tilde{\omega}) & Cos^2\theta(\tilde{\omega}) - Sin^2\theta(\tilde{\omega}) \end{bmatrix}$$

$$\text{and } \left[T_2(\tilde{\omega})\right] = \begin{bmatrix} Cos\theta(\tilde{\omega}) & -Sin\theta(\tilde{\omega}) \\ Sin\theta(\tilde{\omega}) & Cos\theta(\tilde{\omega}) \end{bmatrix}$$

$$[Q_{ij}(\tilde{\omega})]_k = \begin{bmatrix} Q_{11}(\tilde{\omega}) & Q_{12}(\tilde{\omega}) & 0 \\ Q_{12}(\tilde{\omega}) & Q_{22}(\tilde{\omega}) & 0 \\ 0 & 0 & Q_{66}(\tilde{\omega}) \end{bmatrix} \text{ for } i,j = 1,2,6$$

$$\text{and } [Q_{ij}(\tilde{\omega})]_k = \begin{bmatrix} Q_{44}(\tilde{\omega}) & 0 \\ 0 & Q_{55}(\tilde{\omega}) \end{bmatrix} \text{ for } i,j = 4,5$$

where Q_{ij} are the in-plane element of the stiffness matrix. From Hamilton's principle [29], the dynamic equilibrium equation (for free vibration) can be expressed as [30,31].

$$[M_e(\tilde{\omega})]\{\ddot{\delta}_e\} + [K_e(\tilde{\omega})]\{\delta_e\} = 0 \tag{15}$$

where $M_e(\tilde{\omega})$ and $K_e(\tilde{\omega})$ are element mass and stiffness matrices, respectively. Here $[K_e(\tilde{\omega})] = [K_{ela}(\tilde{\omega})] + [K_{geo}(\tilde{\omega})]$ as the sum of element elastic stiffness matrix $[K_{ela}(\tilde{\omega})]$ and geometric stiffness matrix $[K_{geo}(\tilde{\omega})]$. After assembling all the element matrices and the force vectors with respect to the common global coordinates, the resulting equilibrium equation is formulated. Considering randomness of input parameters like temperature, ply-orientation angle, elastic modulus etc., the equation of motion of free vibration system after of assembling with n degrees of freedom can expressed as

$$[M(\tilde{\omega})]\left[\ddot{\delta}\right] + [K(\tilde{\omega})]\{\delta\} = 0 \tag{16}$$

where$\{\delta\}$ denotes the vector of generalized coordinates. The governing equations are derived based on Mindlin's Theory [32] incorporating rotary inertia, transverse shear deformation. The random natural frequencies $[\omega_n(\tilde{\omega})]$ can be calculated employing standard eigenvalue problem [33] and by solving the QR iteration

algorithm. In the present study, an eight noded isoparametric quadratic element with five degrees of freedom at each node (three translations and two rotations) is considered for finite element formulation with respect to laminated composite cantilever plate wherein the shape functions (N_i) are as follows

$$N_i = (1+\xi\xi_i)(1+\varsigma\varsigma_i)(\xi\xi_i+\varsigma\varsigma_i-1)/4 \quad (\text{for } i=1,2,3,4) \tag{17}$$

$$N_i = \left(1-\xi^2\right)(1+\varsigma\varsigma_i)\Big/2 \quad (\text{for } i=5,7) \tag{18}$$

$$N_i = \left(1-\varsigma^2\right)(1+\xi\xi_i)\Big/2 \quad (\text{for } i=6,8) \tag{19}$$

where ς and ξ are the local natural coordinates of the element. The element stiffness matrix is given by

$$[K_e(\tilde{\omega})] = \int_{-1}^{+1}\int_{-1}^{+1} [B]^T[D(\tilde{\omega})][B][J_c]d\xi d\varsigma \tag{20}$$

where, $[B]$ is the strain displacement matrix and $[D(\tilde{\omega})]$ is the random stress-strain matrix. The strain displacement matrix, $[B] = [[B_1], [B_2], \ldots\ldots\ldots [B_8]]$

$$[B_i] = \begin{bmatrix} N_{i,x} & 0 & 0 & 0 & 0 \\ 0 & N_{i,y} & 0 & 0 & 0 \\ N_{i,y} & N_{i,x} & 0 & 0 & 0 \\ 0 & 0 & 0 & N_{i,x} & 0 \\ 0 & 0 & 0 & 0 & N_{i,y} \\ N_{i,y} & -N_{i,x} & 0 & N_{i,y} & N_{i,x} \\ 0 & 0 & N_{i,x} & N_i & 0 \\ 0 & 0 & N_{i,y} & 0 & N_i \end{bmatrix} \tag{21}$$

The element mass matrix is obtained from the Integral

$$[M_e(\tilde{\omega})] = \int_{-1}^{+1}\int_{-1}^{+1} [N]^T[\rho(\tilde{\omega})][N][J_c]d\xi d\varsigma \tag{22}$$

where, $[N]$ is the shape function matrix and $[\rho(\tilde{\omega})]$ is the random inertia matrix. The derivatives of the shape function, N_i with respect to x, y are expressed in term of their derivatives with respect to ξ and ς by the following relationship

$$\begin{bmatrix} N_{i,x} \\ N_{i,y} \end{bmatrix} = [J_c]^{-1}\begin{bmatrix} N_{i,\xi} \\ N_{i,\varsigma} \end{bmatrix} \quad \text{where Jacobian } [J_c] = \begin{bmatrix} \frac{\partial x}{\partial \xi} & \frac{\partial y}{\partial \xi} \\ \frac{\partial x}{\partial \varsigma} & \frac{\partial x}{\partial \varsigma} \end{bmatrix} \tag{23}$$

3. Formulation of GHDMR

The general high dimensional model representation (GHDMR) is important because in real practical applications, the variables are often correlated, for example, the cases wherein the input variables have some relations between them. Here relation can be deterministic or stochastic. For instance, large values of certain input variables may imply large or small values of some other stochastic input variables. Such relation may be controlled by some known or unknown distributions. These correlations are implicitly contained in the collected samples in practice. The GHDMR can construct a proper model for prediction of the random output (say natural frequency) in the stochastic domain. The present approach can treat both independent and correlated input variables, and includes independent input variables as a special case. The role of D-MORPH is to ensure the component functions' orthogonality in hierarchical manner. The present technique decomposes the function $\lambda(S)$ with component functions by input parameters, $S=(S_1,S_2,\ldots,S_{kk})$. As the input parameters are independent in nature, the component functions are specifically projected by vanishing condition. Hence, it has limitation for general formulation. In contrast, a novel numerical analysis with component functions is portrayed in the problem of present context wherein a unified framework for general HDMR dealing with both correlated and independent variables are established. For different input parameters, the output is calculated as [16].

$$\lambda(S) = \lambda_0 + \sum_{i=1}^{kk}\lambda_i(S_i) + \sum_{1\le i<j\le kk}\lambda_{ij}(S_i,S_j) + \ldots\ldots + \lambda_{12\ldots\ldots kk}(S_1,S_2,\ldots\ldots,S_{kk}) \tag{24}$$

$$\lambda(S) = \sum_{u\subseteq kk}\lambda_u(S_u) \tag{25}$$

where λ_0(zeroth order component function) represents the mean value. $\lambda_i(S_i)$ and $\lambda_{ij}(S_i,S_j)$ denote the first and second order component functions, respectively while $\lambda_{12\ldots\ldots kk}(S_1,S_2,\ldots..,S_{kk})$ indicates the residual contribution by input parameters. The subset $u\subseteq\{1,2,\ldots.,kk\}$ denotes the subset where $u\subseteq kk$ for simplicity and empty set, $\Gamma\in u$. As per Hooker's definition, the correlated variables are expressed as,

$$\{\lambda_u(S_u|u\subseteq kk)\} = Argmin_{\{g_u\in L^2(R^u),u\subseteq kk\}}\int\left(\sum_{u\subseteq k}g_u(S_u)-\lambda(S)\right)^2 \times w(S)dS \tag{26}$$

$$\forall u\subseteq kk,\ \ \forall i\in u,\ \ \int\lambda_u(S_u)w(S)dS_i dS_{-u} = 0 \tag{27}$$

and

$$\forall v\subset u,\ \ \forall g_v:\int\lambda_u(S_u)g_v(S_v)w(S)dS = \langle\lambda_u(S_u),g_v(S_v)\rangle = 0 \tag{28}$$

The function $\lambda(S)$ can be obtained from sample data by experiments or by modelling. To minimise the computational cost, the reduction of the squared error can be realised easily. Assuming H in Hilbert space is expanded on the basis $\{h_1, h_2, \ldots, h_{kk}\}$, the bigger subspace $\overline{H}(\supset H)$ is expanded by extended basis $\{h_1, h_2, \ldots, h_{kk}, h_{kk+1}, \ldots, h_m\}$. Then $\overline{H}$ can be decomposed as

$$\overline{H} = H\oplus H^{\perp} \tag{29}$$

where $H^{\perp}$ denotes the complement subspace (orthogonal) of H [34] within $\overline{H}$. In the past work [35–37], the component functions are calculated from basis functions. The component functions of Second order HDMR expansion are estimated from basis functions $\{\varphi\}$ as [21].

$$\lambda_i(S_i) \approx \sum_{r=1}^{kk}\alpha_r^{(0)i}\varphi_r^i(S_i) \tag{30}$$

$$\lambda_{ij}(S_i,S_j) \approx \sum_{r=1}^{kk}\left[\alpha_r^{(i\,j)i}\varphi_r^i(S_i)+\alpha_r^{(i\,j)j}\varphi_r^j(S_j)\right] + \sum_{p=1}^{l} \times \sum_{q=1}^{l}\beta_{pq}^{(0)ij}\varphi_p^i(S_i)\varphi_q^j(S_j) \tag{31}$$

i.e., the basis functions of $\lambda_{ij}(S_i,S_j)$ contain all the basis functions used in $\lambda_i(S_i)$ and $\lambda_j(S_j)$.

The HDMR expansions at N_{samp} sample points of S can be represented as a linear algebraic equation system

$$\Gamma J = \widehat{R} \tag{32}$$

where Γ denotes a matrix $(N_{samp} \times \tilde{t})$ whose elements are basis functions at the N_{samp} values of S; J is a vector with $\tilde{t}$ dimension of all unknown combination coefficients; $\widehat{R}$ is a vector with N_{samp}-dimension wherein l-th element is $\lambda(S^{(l)})$-λ_0. $S^{(l)}$ denotes the l-th sample of S, and λ_0 represents the average value of all $\lambda(S^{(l)})$. The regression equation for least squares of the above equation can be expressed as

$$\frac{1}{N_{samp}}\Gamma^T\Gamma J = \frac{1}{N_{samp}}\Gamma^T\widehat{R} \tag{33}$$

Due to the use of extended bases, some rows of the above equation are identical and can be removed to give an underdetermined algebraic equation system

$$AJ = \widehat{V} \tag{34}$$

It has many of solutions for J composing a manifold $Y \in \Re^{\tilde{t}}$. Now the task is to find a solution J from Y to force the HDMR component functions satisfying the hierarchical orthogonal condition. D-MORPH regression provides a solution to ensure additional condition of exploration path represented by differential equation

$$\frac{dJ(l)}{dl} = \chi v(l) = \left(I_t - A^+A\right)v(l) \tag{35}$$

wherein χ denotes orthogonal projector ensuring

$$\chi^2 = \chi \text{ and } \chi^T = \chi \tag{36}$$

$$\chi = \chi^2 = \chi^T\chi \tag{37}$$

The free function vector may be selected to ensure the wide domain for $J(l)$ as well as to simultaneously reduce the cost $\kappa(J(l))$ which can be expressed as

$$v(l) = -\frac{\partial\kappa(J(l))}{\partial J} \tag{38}$$

Then we obtain

$$\begin{aligned}\frac{\partial\kappa(J(l))}{\partial l} &= \left(\frac{\partial\kappa(J(l))}{\partial J}\right)^T\frac{\partial J(l)}{\partial l} = \left(\frac{\partial\kappa(J(l))}{\partial J}\right)^T Pv(l)\\ &= -\left(P\frac{\partial\kappa(J(l))}{\partial J}\right)^T\left(P\frac{\partial\kappa(J(l))}{\partial J}\right) \le 0\end{aligned} \tag{39}$$

The cost function can be expressed in quadratic form as

$$\kappa = \frac{1}{2}J^TBJ \tag{40}$$

where B denotes the positive definite symmetric matrix and J_∞ can be expressed as

$$J_\infty = V_t\left(U_{\tilde{t}-r}^TV_{\tilde{t}-r}\right)^{-1}U_{\tilde{t}-r}^TA^+\widehat{V} \tag{41}$$

where the last columns $(\tilde{t}-r)$ of U and V are denoted as $U_{\tilde{t}-r}$ and $V_{\tilde{t}-r}$ which can found by decomposition of χB [38].

$$\chi B = U\begin{bmatrix}\bar{S}_r & 0\\ 0 & 0\end{bmatrix}V^T \tag{42}$$

This unique solution J_∞ in Y indicates the minimized cost function. D-MORPH regression is used to find the J which ensures the HDMR component functions' orthogonality in hierarchical manner. The construction of the corresponding cost function κ can be found in previous literature [16].

4. Random input representation

The random input parameters such as ply-orientation angle and temperature in each layer of laminate are considered for composite cantilever plates. It is assumed that the distribution of random input parameters exists within a certain band of tolerance with their crisp values. The cases wherein the input variables considered in each layer of laminate are as follows:

(a) Variation of ply-orientation angle only: $\theta(\tilde{\omega}) = \{\theta_1\ \theta_2\ \theta_3 \ldots\ldots\theta_i\ldots\ldots\theta_l\}$
(b) Variation of longitudinal elastic modulus only: $E_1(\tilde{\omega}) = \{E_{1(1)}\ E_{1(2)}\ E_{1(3)}\ldots\ldots E_{1(i)}\ldots\ldots E_{1(l)}\}$
(c) Variation of shear modulus only: $G_{12}(\tilde{\omega}) = \{G_{12(1)}\ G_{12(2)}\ G_{12(3)}\ldots G_{12(i)}\ldots G_{12(l)}\}$
(d) Variation of temperature only: $T(\tilde{\omega}) = \{T_{(1)}\ T_{(2)}\ T_{(3)}\ldots\ldots T_{(i)}\ldots\ldots T_{(l)}\}$
(e) Combined variation of ply orientation angle, elastic modulus, shear modulus and temperature: $[\theta, E_1, G_{12}, T(\tilde{\omega})] = [(\theta_1\ldots\theta_l), (E_{1(1)}\ldots E_{1(l)}), (G_{12(1)}\ldots G_{12(l)}), (T_{(1)}\ldots T_{(l)})]$

where θ_i, $E_{1(i)}$, $G_{12(i)}$ and $T_{(i)}$ are the ply orientation angle, temperature, respectively and 'l' denotes the number of layer in the laminate. In present study, $\pm5^\circ$ variation for ply orientation angle, $\pm10\%$ volatility in material properties and ±25 K tolerance for temperature, respectively are considered from their respective deterministic values. Fig. 2 presents the flowchart of frequency responses using GHDMR with D-MORPH. It is worth mentioning that material properties such as E_1 and G_{12} are considered as temperature dependant in the present study. Thus in case of the combined variation of ply orientation angle, elastic modulus, shear modulus and temperature, correlated input variables are needed to be mapped for natural frequencies as discussed in section-1.

5. Results and discussion

The present study considers four layered graphite-epoxy angle-ply $[(\theta^\circ/\text{-}\theta^\circ/\theta^\circ/\text{-}\theta^\circ)]$ and cross-ply $(0^\circ/90^\circ/0^\circ/90^\circ)$ composite cantilever plates. An eight noded isoparametric plate bending element is considered for finite element formulation. Due to paucity of space, only a few important representative results are furnished. Table 1 presents the convergence study of non-dimensional fundamental natural frequencies of three layered graphite-epoxy untwisted composite plates [39]. Table 2 presents the non-dimensional natural frequencies for simply-supported graphite-epoxy symmetric cross-ply composite plates [40]. In both the cases, close agreement with benchmarking results are obtained at (6×6) mesh size. Material properties and their variation with temperature [41] are furnished in Table 3. Considering mean temperature $T = 300$ K and thickness $t = 0.004$ m, the deterministic values of material properties are considered as $E_1 = E_2 = 15.4$ GPa, $\nu = 0.43$, $G_{12} = G_{13} = G_{23} = 3.56$ GPa, $\rho = 1660$ kg/m^3. The present GHDMR methodology is employed to find a predictive and representative surrogate model relating each natural frequency to a number of input variables. The present surrogate models are used to determine the first three natural frequencies corresponding to given

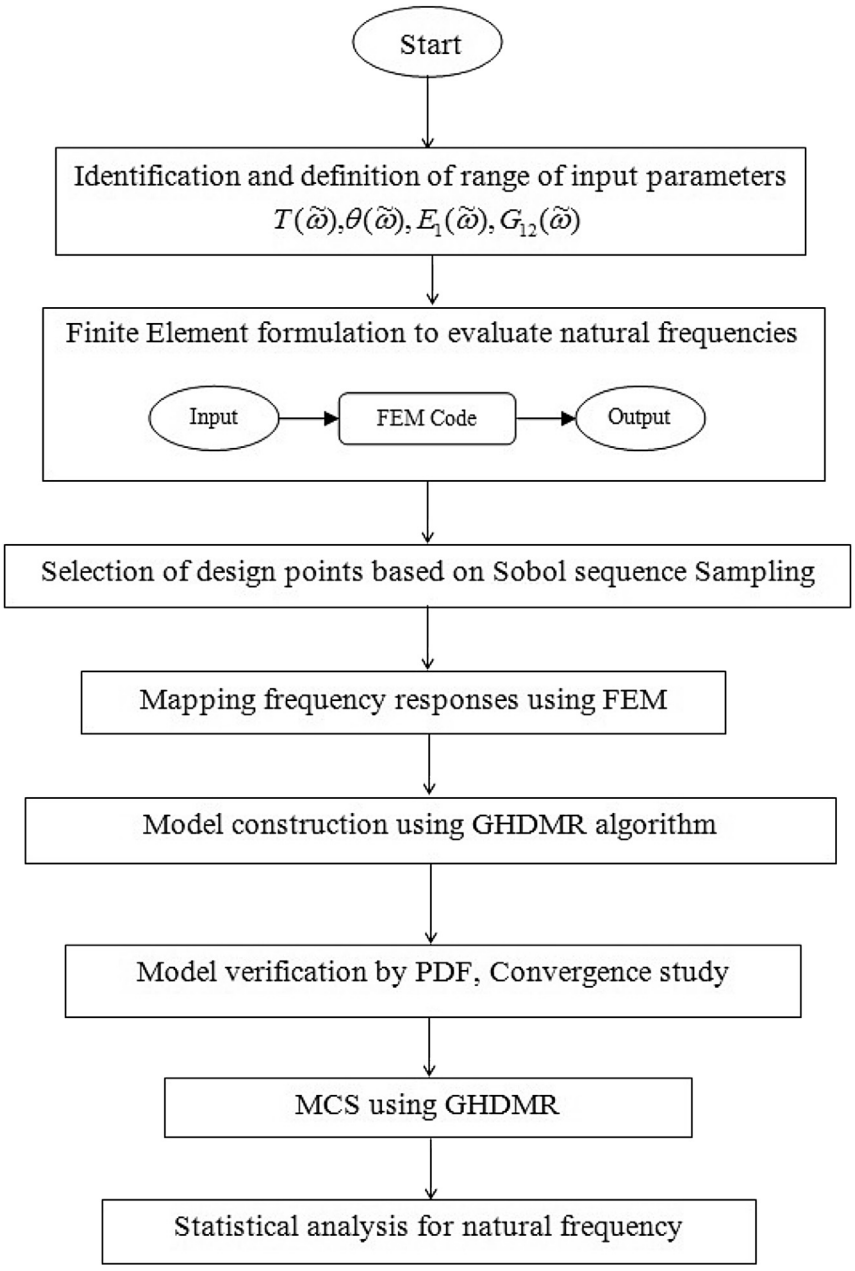

Fig. 2. Flowchart of frequency responses using GHDMR with D-MORPH.

values of input variables, instead of time-consuming deterministic finite element analysis. The probability density function is plotted as the benchmark of bottom line results. Due to paucity of space, only a few important representative results are furnished. The variation of temperature is scaled in the range with the lower and the upper limit (tolerance limit) as ±25 K with respective mean values while for ply orientation angle as within ±5° fluctuation (as per standard of composite manufacturing industry) with respective deterministic values. Both angle-ply and cross-ply composite cantilever plates are considered for the present analysis.

Fig. 3 presents the scatter plot which establishes the accuracy of present model with respect to original finite element model corresponding to random fundamental natural frequencies for combined variation of temperature and ply orientation angle. Table 4

Table 1
Convergence study for non-dimensional fundamental natural frequencies [$\omega = \omega_n L^2 \sqrt{(\rho/E_1 t^2)}$] of three layered ($\theta^\circ/-\theta^\circ/\theta^\circ$) graphite-epoxy untwisted composite plates, a/b = 1, b/t = 100, considering $E_1 = 138$ GPa, $E_2 = 8.96$ GPa, $G_{12} = 7.1$ GPa, $\nu_{12} = 0.3$.

Ply angle, θ	Present FEM (4 × 4)	Present FEM (6 × 6)	Present FEM (8 × 8)	Present FEM (10 × 10)	Qatu and Leissa [39]
0°	1.0112	1.0133	1.0107	1.004	1.0175
45°	0.4556	0.4577	0.4553	0.4549	0.4613
90°	0.2553	0.2567	0.2547	0.2542	0.2590

Table 2
Non-dimensional natural frequencies [$\omega = \omega_n a^2 \sqrt{(\rho/E_2 t^2)}$] for simply-supported graphite-epoxy symmetric cross-ply (0°/90°/90°/0°) composite plates considering a/b = 1, T = 325 K, a/t = 100.

Frequency	Present FEM (4 × 4)	Present FEM (6 × 6)	Present FEM (8 × 8)	Present FEM (10 × 10)	Sai Ram and Sinha [40]
1	8.041	8.061	8.023	8.001	8.088
2	18.772	19.008	18.684	18.552	19.196
3	38.701	38.981	38.597	38.443	39.324

Table 3
Material properties of glass/epoxy lamina at different temperatures, $E_1 = E_2$, $G_{12} = G_{13} = G_{23}$, mass density (ρ) = 1660 kg/m^3, ν = 0.43 [41].

Material properties (GPa)	Temperature (K)						
	125	150	200	250	300	350	400
E_1	15.4	15.4	15.4	15.4	15.4	14.93	14.7
G_{12}	3.56	3.56	3.56	3.56	3.56	3.51	3.48

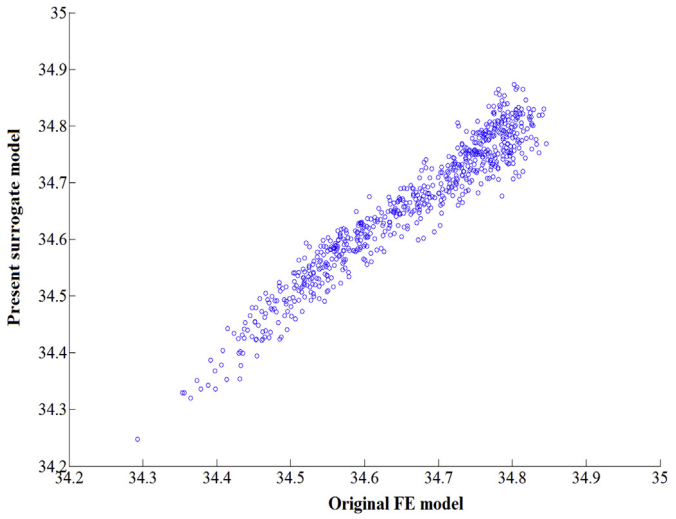

Fig. 3. Scatter plot for present surrogate model with respect to original FE model of fundamental natural frequencies for combined variation of ply-orientation angle and temperature of graphite-epoxy angle-ply (45°/−45°/45°/−45°) composite cantilever plate, considering $E_1 = E_2 = 15.4$ GPa, $G_{12} = G_{13} = G_{23} = 3.56$ GPa,$T = 300$ K,$\rho = 1660$ kg/m^3, $t = 0.004$ m, $\nu = 0.43$.

presents the convergence study of present method compared to direct Monte Carlo simulation (MCS) for first three natural frequencies due to individual variation of ply-orientation angle and temperature of angle-ply (45°/−45°/45°/−45°) composite cantilever plate while Table 5 represents the convergence study of the present method with direct MCS for first three natural frequencies due to combined variation of temperature, ply-orientation angle, elastic modulus and shear modulus of angle-ply (45°/−45°/45°/−45°) composite cantilever plate. Fig. 4(a–i) presents the comparative probability density function plot with respect to first three natural frequencies due to individual and combined variation of stochastic input parameters of angle-ply (45°/−45°/45°/−45°) composite cantilever plate for both MCS as well as present method. In present analysis, a sample size of 64 is considered for layerwise individual variation of stochastic input parameters, while due to increment of number of input variables for combined random variation, the subsequent sample size of 512 is adopted to meet the convergence criteria. Here, although the same sampling size as in direct MCS (10,000 samples) is considered, the number of actual FE analysis is much less compared to original MCS and is equal to number representative sample required to construct the surroagte model. The surrogate model is formed on which the full sample size of direct MCS is conducted. Hence, the computational time and effort expressed in terms of FE calculation is reduced compared to full scale direct MCS. This provides an efficient affordable way for simulating the uncertainties in natural frequency.

A comparative study on variation of stochastic natural frequencies is carried out for angle-ply (45°/−45°/45°/−45°) and cross-ply (0°/90°/0°/90°) composite cantilever plate due to individual variation of elastic modulus, shear modulus as furnished in Fig. 5(a–f). From Fig. 5, it is observed that the mean fundamental natural frequency for angle-ply laminate is found to be slightly lower than that of the same for cross-ply laminate while a significant higher mean values are obtained at second and third modes for angle-ply compared to cross-ply. Considering only variation of temperature of angle-ply (45°/−45°/45°/−45°) and cross-ply (0°/90°/0°/90°) composite cantilever plate, the probability density

Table 4
Convergence study of first three natural frequencies due to individual variation of ply-orientation angle and temperature of angle-ply (45°/−45°/45°/−45°) composite cantilever plate considering $E_1 = E_2 = 15.4$ GPa, $G_{12} = G_{13} = G_{23} = 3.56$ GPa, $\rho = 1660$ kg/m^3, $t = 0.004$ m, $\nu = 0.43$, $T_{mean} = 300$ K.

Parameter	Values	f_1				f_2				f_3			
		MCS (10,000)	Present method (sample run)			MCS (10,000)	Present method (sample run)			MCS (10,000)	Present method (sample run)		
			32	64	128		32	64	128		32	64	128
$\theta(\tilde{\omega})$	Max	34.8601	34.8999	34.8664	34.8783	98.1667	98.4748	98.6176	98.5928	216.7606	217.8250	216.7751	217.1431
	Min	34.2870	34.2531	34.2767	34.2941	84.9534	84.8309	84.8548	84.9552	205.8846	204.4143	205.7557	206.1325
	Mean	34.6546	34.6468	34.6509	34.6561	92.0607	92.0099	92.0172	92.0485	213.6560	213.4836	213.5772	213.6981
	SD	0.1061	0.1095	0.1068	0.1068	2.4501	2.4564	2.4550	2.4673	2.0449	2.1606	2.0635	2.0517
$T(\tilde{\omega})$	Max	34.6904	34.6996	34.6932	34.6922	93.0976	93.1461	93.1307	93.1468	214.4427	214.6334	214.5056	214.4707
	Min	34.4488	34.4591	34.4536	34.4554	88.24453	88.3375	88.3098	88.3482	209.4478	209.5902	209.5364	209.5452
	Mean	34.5872	34.5879	34.5877	34.5872	90.7581	90.7659	90.7653	90.7634	212.3069	212.3222	212.3173	212.3069
	SD	0.0422	0.0428	0.0429	0.04287	0.8561	0.8707	0.8710	0.8686	0.8882	0.9011	0.9034	0.9016

Table 5
Convergence study of the present method with direct Monte Carlo simulation (MCS) for first three natural frequencies due to combined variation of temperature, ply-orientation angle, elastic modulus and shear modulus of angle-ply (45°/−45°/45°/−45°) composite cantilever plate.

Frequency	Method	Sample size	Parameters			
			Max	Min	Mean	Standard deviation
f_1	MCS	10,000	34.8508	34.2855	34.5996	0.1187
	Present method	32	34.9831	34.0428	34.5836	0.1019
		64	34.9002	34.2454	34.5978	0.0985
		128	35.0770	34.0130	34.6000	0.1403
		256	34.8492	34.2701	34.5999	0.1187
		512	34.8511	34.2638	34.5997	0.1195
		1024	34.8521	34.2628	34.5996	0.1198
f_2	MCS	10,000	96.4222	84.7779	90.7088	2.4025
	Present method	32	99.0099	79.0589	90.4359	2.0766
		64	96.9819	84.2358	90.6973	1.9971
		128	97.0225	83.4915	90.6970	2.4065
		256	96.3939	84.6852	90.7179	2.4068
		512	96.4816	84.4608	90.7116	2.4215
		1024	96.4883	84.4624	90.7110	2.4225
f_3	MCS	10,000	216.6953	205.2277	212.2366	2.4307
	Present method	32	219.6954	200.6440	211.9285	2.1035
		64	218.1019	204.7512	212.1888	1.9985
		128	224.9086	197.1597	212.2513	3.3649
		256	216.7612	205.1236	212.2363	2.4305
		512	216.7192	204.7821	212.2321	2.4455
		1024	216.7172	204.7808	212.2319	2.4414

function (PDF) with respect to first three natural frequencies are plotted in Fig. 6(a–f) wherein it is found that as the temperature increases the variabilities of first three natural frequencies of angle-ply laminate are increased and the probability density function curves become more steeper as the temperature increases. This can be attributed to the fact that due to rise in temperature influences the thermo-mechanical loading due to random variation leading to change in the system properties. In contrast, the reverse trend is identified for cross-ply laminated composite plates due to reduction effect of 0° and 90° on effective stiffness of the laminate. On the other hand, Fig. 7(a–c) presents the ply level quantification of uncertainty in first three natural frequencies in terms of Probability density function for angle-ply [$(\theta^\circ/-\theta^\circ/\theta^\circ/-\theta^\circ)$ where θ = Ply orientation angle] and cross-ply (0°/90°/0°/90°) composite cantilever plate. Due to random variation of ply orientation angle, the elastic stiffness of the laminated composite plate is found to be

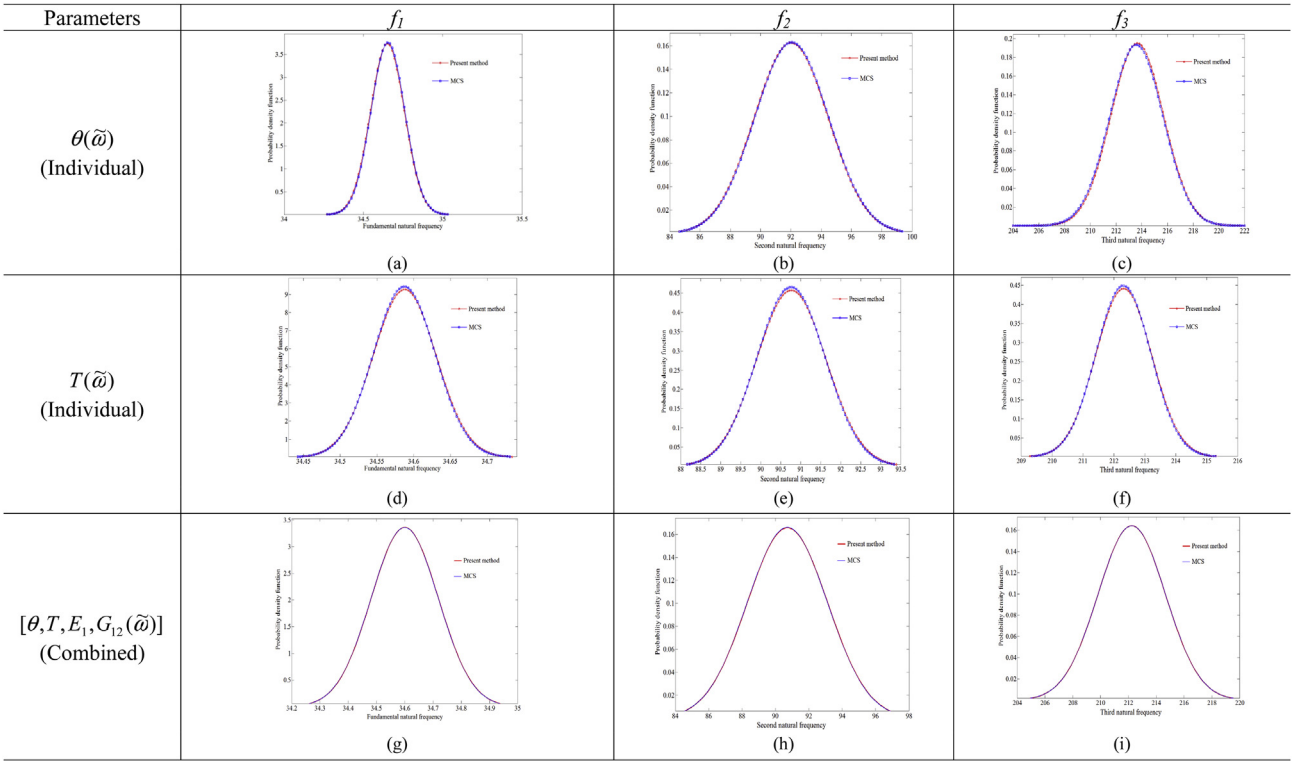

Fig. 4. **(a–i)** Probability density function with respect to first three natural frequencies (Hz) due to individual and combined variation of ply orientation angle, elastic modulus, shear modulus and temperature of angle-ply (45°/−45°/45°/−45°) composite cantilever plate at mean temperature (T_{mean}) = 300 K.

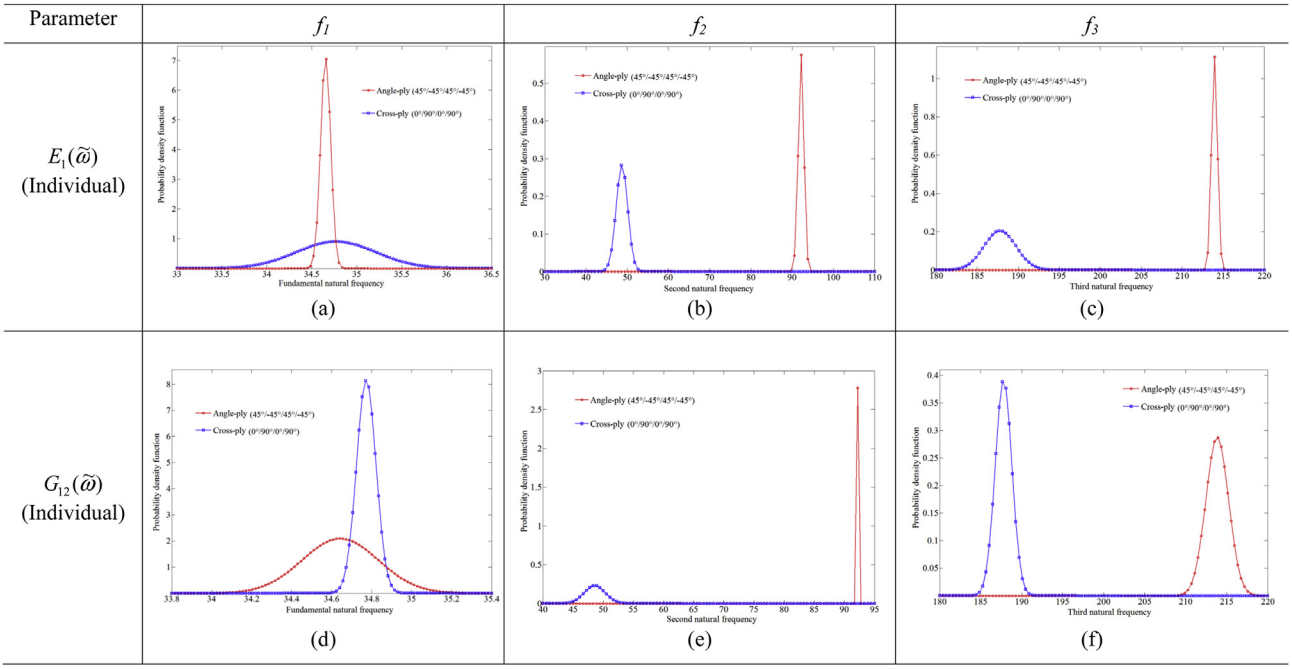

Fig. 5. **(a–f)** Probability density function with respect to first three natural frequencies (Hz) due to individual variation of elastic modulus, shear modulus of angle-ply (45°/−45°/45°/−45°) and cross-ply (0°/90°/0°/90°) composite cantilever plate at mean temperature (T_{mean}) = 300 K.

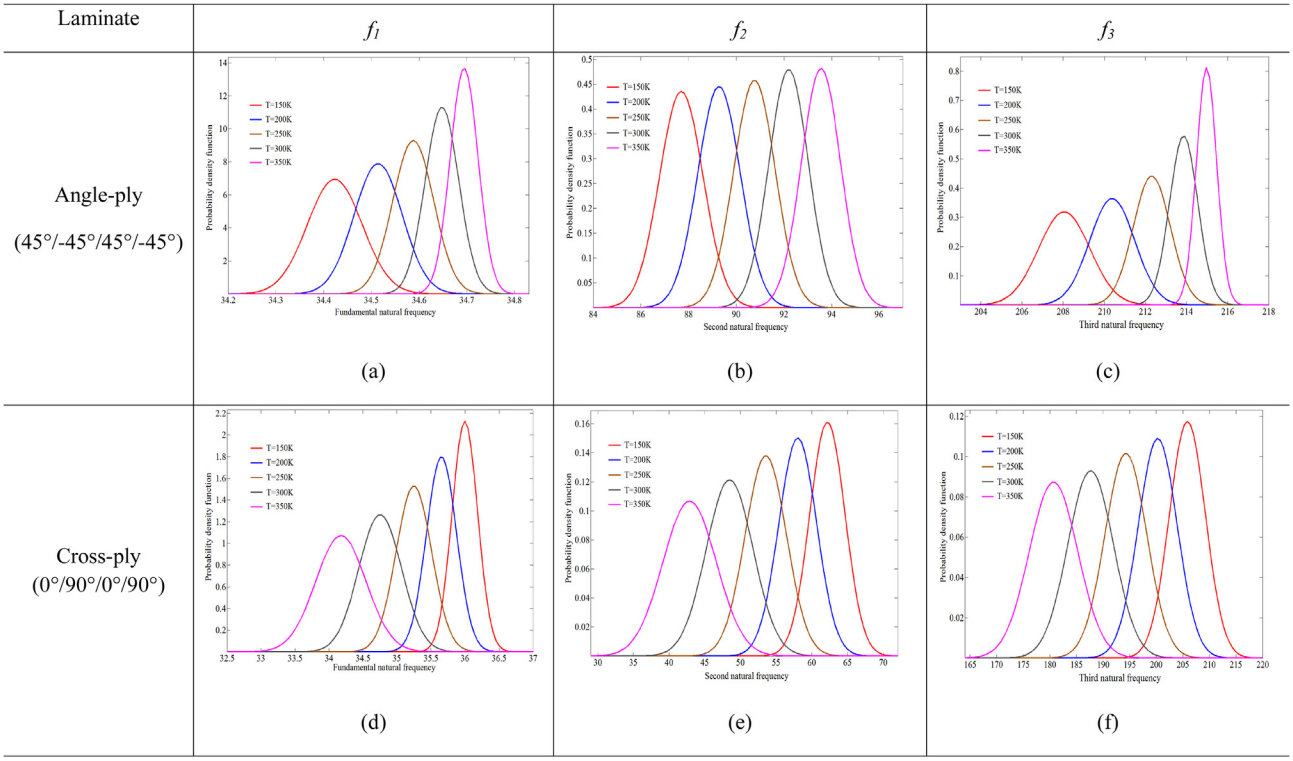

Fig. 6. **(a–f)** Probability density function with respect to first three natural frequencies (Hz) due to individual variation of temperature of angle-ply (45°/−45°/45°/−45°) and cross-ply (0°/90°/0°/90°) composite cantilever plate.

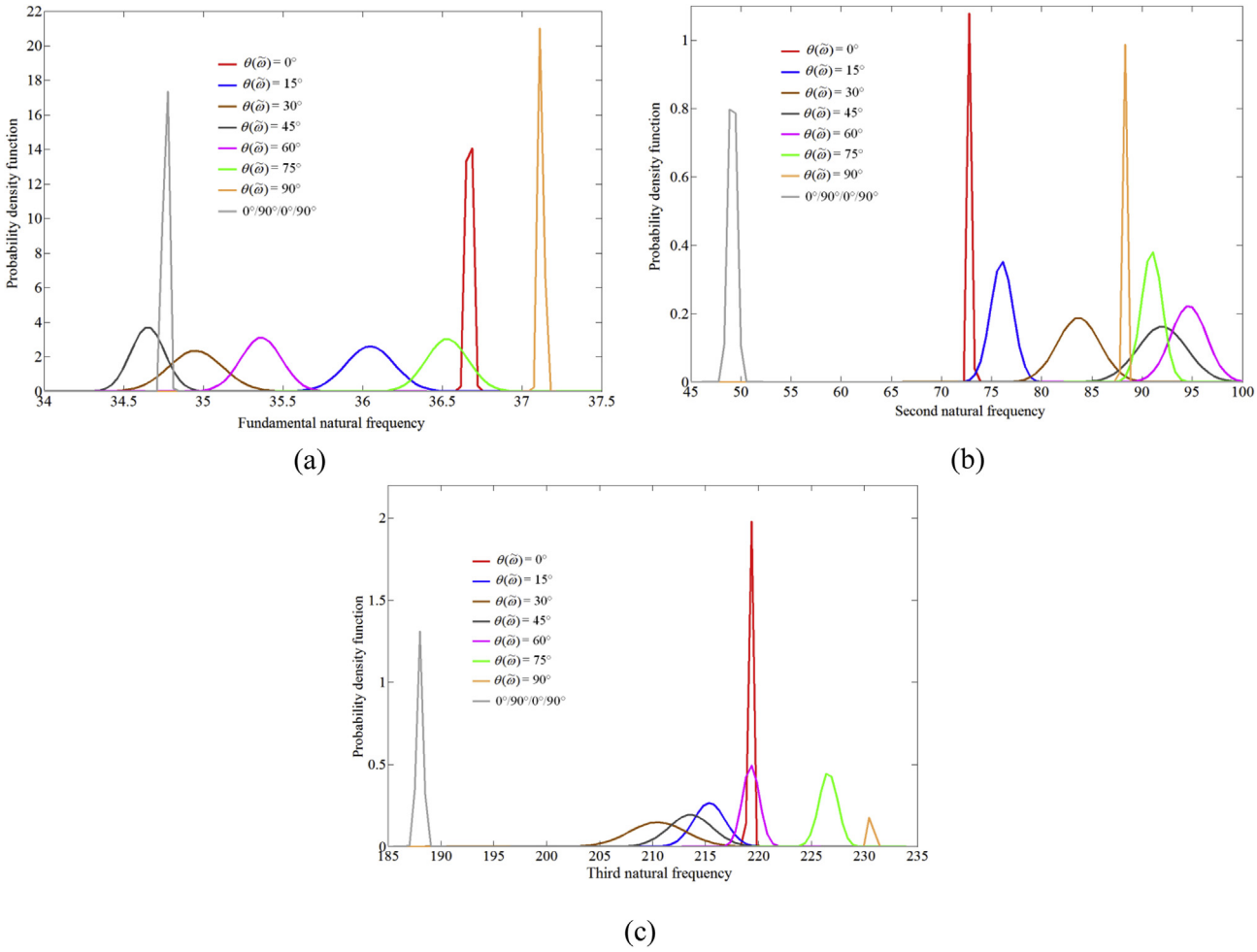

Fig. 7. (a–c) Probability density function with respect to first three natural frequencies (Hz) due to individual variation of ply orientation angle of angle-ply [$(\theta^\circ/-\theta^\circ/\theta^\circ/-\theta^\circ)$ where θ=0°,15°,30°,45°,60°,75° and 90°] and cross-ply(0°/90°/0°/90°) composite cantilever plate at mean temperature (T_{mean}) = 300 K.

varied which in turn influence the frequency responses irrespective of laminate configuration. The effect of combined variation of input parameters is also carried out in addition to individual variation of inputs in conjunction to stochastic natural frequencies for composite laminated plates as furnished in Fig. 8(a–c). The ply orientation angle, elastic modulus, shear modulus and temperature of angle-ply (45°/−45°/45°/−45°) and cross-ply (0°/90°/0°/90°) are considered as random input variables wherein the upper and lower bounds of volatility in natural frequencies are found to be wider than that of individual variation of inputs irrespective of laminate configuration. This corroborates with the fact that the combined effect of random input parameters leads to increase the variation in outputs compared to individual cases.

In the present study, the relative coefficient of variance (RCV) (normalized mean to standard deviation ratio) due to variation of temperature is also quantified for each layer for angle-ply and cross-ply laminate as furnished in Fig. 9(a,b). The two outer-most layers of the angle-ply laminate is found to be most sensitive to temperature variation for first three modes while the maximum sensitiveness of temperature is observed only at bottom layer of the cross-ply laminate. In contrast, the least sensitivity to temperature variation is identified at third intermediate layer for first three modes irrespective of laminate configuration. The layerwise ply-level sensitiveness to temperature variation for fundamental mode is studied to map the sensitivity of each layer due to the influence of ply orientation angle on variation of temperature as furnished in Fig. 10(a–d). The least sensitivity is observed at $\theta(\tilde{\omega}) = 45^\circ$ for outer layers of the angle-ply laminate.

6. Conclusions

This present study illustrates the layer-wise thermal uncertainty propagation with laminated composite plates. The ranges of variation in first three natural frequencies are analyzed considering both individual and combined stochasticity of input parameters. A generalized high dimensional model representation (GHDMR) model in conjunction with diffeomorphic modulation under observable response preserving homotopy (D-MORPH) regression is employed to map the input parameters (both correlated and uncorrelated) and natural frequencies. After utilizing the aforementioned surrogate modelling approach, the number of finite element simulations is found to be exorbitently reduced compared to original Monte Carlo simulation without compromising the accuracy of results. The computational expense is reduced by (1/156) times (individual stochasticity) and (1/19) times (combined stochasticity) of original Monte Carlo simulation. It is observed that as the temperature increases the variabilities of first three natural frequencies of angle-ply laminate are increased

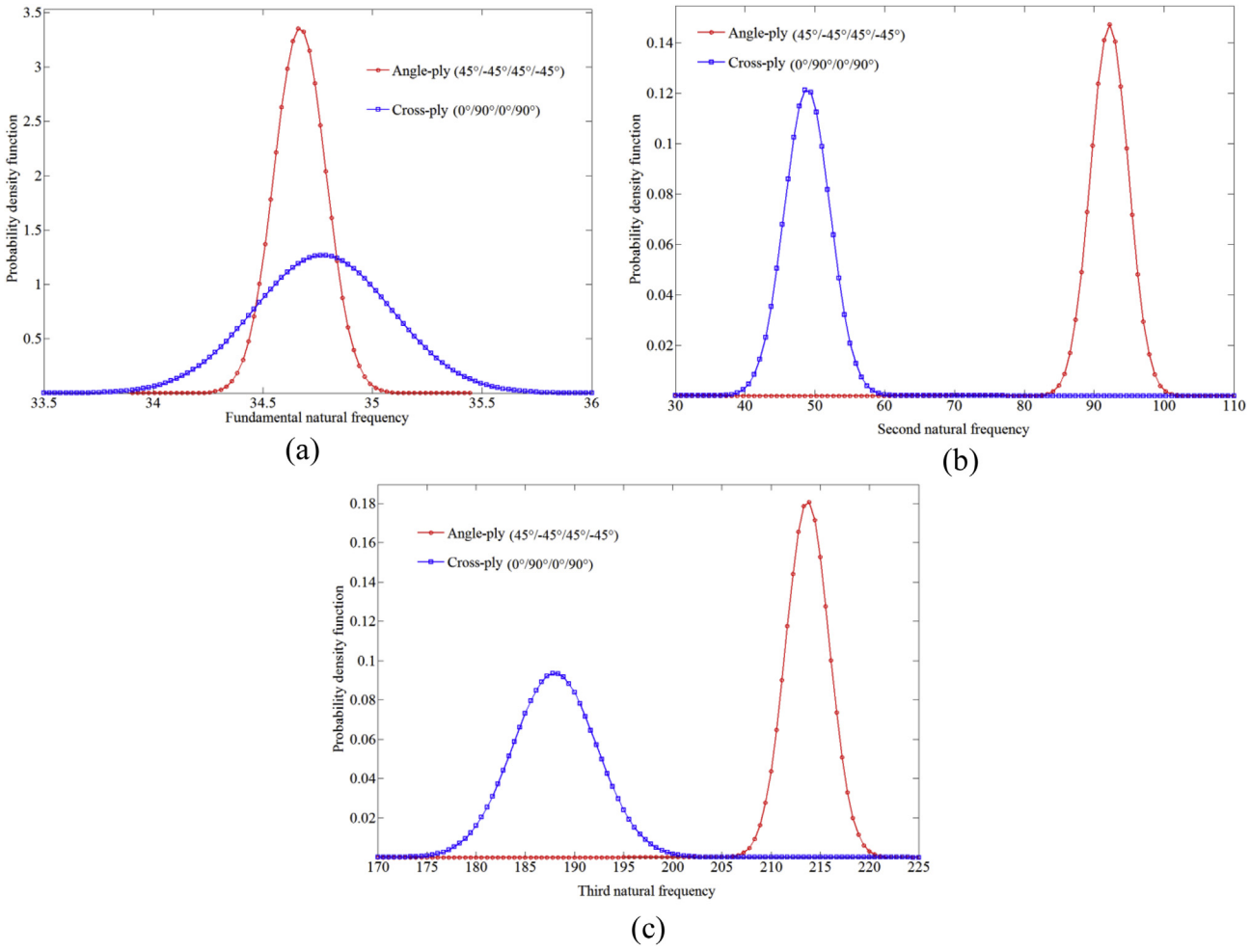

Fig. 8. **(a–c)** Probability density function with respect to first three natural frequencies (Hz) due to combined variation of ply orientation angle, elastic modulus, shear modulus and temperature of angle-ply (45°/−45°/45°/−45°) and cross-ply(0°/90°/0°/90°) composite cantilever plate at mean temperature (T_{mean}) = 300 K.

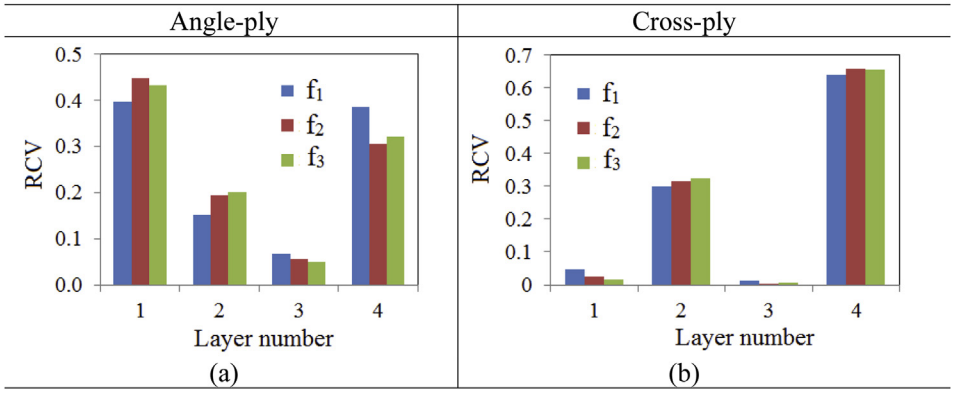

Fig. 9. **(a,b)** Relative coefficient of variance (RCV) offirst three natural frequencies due to variation of temperature (layerwise) for angle-ply (45°/−45°/45°/−45°) and cross-ply(0°/90°/0°/90°) composite cantilever plate at mean temperature (T_{mean}) = 300 K.

and the probability density function become steeper. The two outer-most layers of the angle-ply laminate is found to be most sensitive to temperature variation for first three modes while the maximum sensitivity of temperature is observed at bottom layer of the cross-ply laminate. It is found that stochastic variation of temperature influences the natural frequencies and thus it is a crucial design parameter from the operational safety and serviceability point of view. The numerical results obtained in this study provide a comprehensive idea for design and control of laminated composite structures. The results presented could serve as reference solutions to explore more complex systems in future course of research.

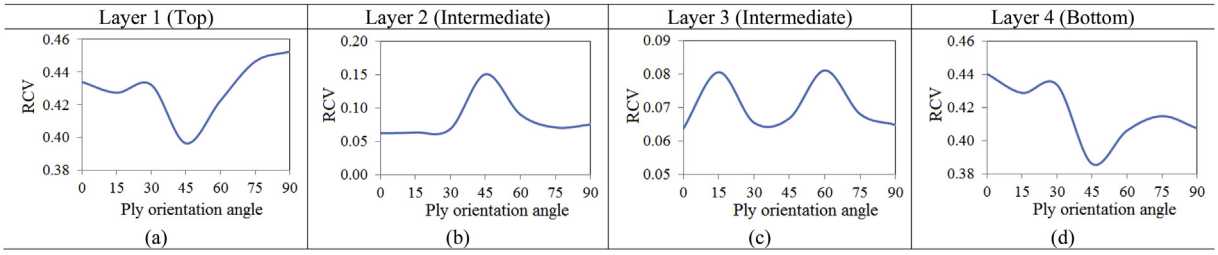

Fig. 10. (a–d) Relative coefficient of variance (RCV) of fundamental mode due to variation of temperature (layerwise) for angle-ply ($\theta^\circ/-\theta^\circ/\theta^\circ/-\theta^\circ$) ($\theta$ = Ply orientation angle) composite cantilever plate at mean temperature (T_{mean}) = 300 K.

Acknowledgement

HR and GL acknowledge the support of ONR, USA with account number N00014-11-1-0716. SA acknowledges the support of Royal Society of London through the award of Wolfson Research Merit award.

References

[1] Whitney JM, Ashton JE. Effect of environment on the elastic response of layered composite plates. AIAA J 1971;9:1708–13.
[2] Strife JR, Prewo KM. The thermal expansion behavior of unidirection and bidirectional kevlar/epoxy composites. J Compos Mater 1979;13:265–77.
[3] Bowles DE, Tompkins SS. Prediction of coefficients of thermal expansion for unidirectional composite. J Compos Mater 1989;23:370–81.
[4] Seng LK, Earn TT, Shim VPW. Hygrothermal analysis of woven-fabric composite plates. Compos Part B Eng 1997;28(5–6):573–81.
[5] Park J-S, Kim J-H, Moon S-H. Thermal post-buckling and flutter characteristics of composite plates embedded with shape memory alloy fibers. Compos Part B: Eng 2005;36(8):627–36.
[6] SaiRam KS, Sinha PK. Hygrothermal effects on the buckling of laminated composite plates. Compos Struct 1992;21:233–47.
[7] Wosu SN, Hui David, Daniel L. Hygrothermal effects on the dynamic compressive properties of graphite/epoxy composite material. Compos Part B Eng 2012;43(3):841–55.
[8] Shen HS. Thermal post buckling behaviour of imperfect shear deformable laminated plates with temperature-dependent properties. Comput Methods Appl Mech Eng 2001;190:5377–90.
[9] Nawab Y, Jacquemin F, Casari P, Boyard N, Borjon-Piron Y, Sobotka V. Study of variation of thermal expansion coefficients in carbon/epoxy laminated composite plates. Compos Part B: Eng 2013;50:144–9.
[10] Shariyat M. Thermal buckling analysis of rectangular composite plates with temperature-dependent properties based on a layer wise theory. Thin-Walled Struct 2007;45(4):439–52.
[11] Pandey R, Shukla KK, Jain A. Thermo-elastic stability analysis of laminated composite plates, an analytical approach. Commun Nonlinear Sci Numer Simulat 2008;14(4):1679–99.
[12] Fazzolari FA, Carrera E. Free vibration analysis of sandwich plates with anisotropic face sheets in thermal environment by using the hierarchical trigonometric Ritz formulation. Compos Part B Eng 2013;50:67–81.
[13] Abdelnaser AS, Singh MP. Random response of antisymmetric angle-ply composite plates with levy boundary conditions. Compos Part B Eng 1993;3(9):817–33.
[14] Dai Xin-Jin, Lin Jia-Hao, Chen Hao-Ran, Williams FW. Random vibration of composite structures with an attached frequency-dependent damping layer. Compos Part B Eng 2008;39(2):405–13.
[15] Shaw A, Sriramula S, Gosling PD, Chryssanthopoulos MK. A critical reliability evaluation of fibre reinforced composite materials based on probabilistic micro and macro-mechanical analysis. Compos Part B Eng 2010;41(6):446–53.
[16] Li Genyuan, Rabitz Herschel. General formulation of HDMR component functions with independent and correlated variables. J Math Chem 2012;50:99–130.
[17] Dey S, Mukhopadhyay T, Adhikari S. Stochastic free vibration analysis of angle-ply composite plates – a RS-HDMR approach. Compos Struct 2015. http://dx.doi.org/10.1016/j.compstruct.2014.09.057.
[18] Dey P, Sheikh AH, Sengupta D. A new element for the analysis of composite plates. Finite Elem Analysis Des 2014;82:62–71.
[19] Shanmugam V, Penmetsa R, Tuegel E, Clay S. Stochastic modeling of delamination growth in unidirectional composite DCB specimens using cohesive zone models. Compos Struct 2013;102:38–60.
[20] Rabitz H, Alis ÖF, Shorter J, Shim K. Efficient input output model representations. Comput Phys Comm 1999;117:11–20.
[21] Li G, Hu J, Wang SW, Georgopoulos PG, Schoendorf J, Rabitz H. Random sampling-high dimensional model representation (RS-HDMR) and orthogonality of its different order component functions. J Phys Chem A 2006;110:2474–85.
[22] Li G, Wang SW, Rosenthal C, Rabitz H. High dimensional model representations generated from low dimensional data samples. I. mp-Cut-HDMR. J Math Chem 2001;30:1–30.
[23] Li G, Schoendorf J, Ho TS. Multicut-HDMR with an application to an ionospheric model. J Comp Chem 2004;25:1149–56.
[24] Li G, Artamonov M, Rabitz H, Wang SW, Georgopoulos PG, Demiralp M. High dimensional model representations generated from low order terms – lp-RS-HDMR. J Comput Chem 2003;24:647–56.
[25] Kollar Laszlo P, Springer George S. Mechanics of composite structures. New York, USA: Cambridge University Press; 2009.
[26] Yang PC, Norris CH, Stavsky Y. Elastic wave propagation in heterogeneous plates. Int J Solids Struct 1966;2:665–84.
[27] Jones RM. Mechanics of composite materials. Washington DC: McGraw-Hill; 1975.
[28] Tsai SW, Hahn HT. Introduction to composite materials. Westport, Connecticut: Technomic; 1980.
[29] Meirovitch L. Dynamics and control of structures. New York: J.Wiley & Sons; 1992.
[30] Dey S, Karmakar A. Natural frequencies of delaminated composite rotating conical shells – a finite element approach. Finite Elem Analysis Des 2012;56:41–51.
[31] Dey S, Mukhopadhyay T, Adhikari S. Stochastic free vibration analyses of composite shallow doubly curved shells – a Kriging model approach. Compos Part B: Eng 2015;70:99–112.
[32] Cook Robert D, Malkus David S, Plesha Michael E, Witt Robert J. Concepts and applications of finite element analysis. 4th ed. John Wiley & Sons; 2001 [edition].
[33] Bathe KJ. Finite element Procedures in engineering analysis. New Delhi: PHI; 1990.
[34] Deutsch F. Best approximation in inner product space. New York: Springer; 2000.
[35] Li G, Wang SW, Rabitz H, Wang S, Jáffe PR. Global uncertainty assessments by high dimensional model representations (HDMR). Chem Eng Sci 2002;57:4445–60.
[36] Wang SW, Levy II H, Li G, Rabitz H. Fully equivalent operational models for atmospheric chemical kinetics within global chemistry-transport models. J Geophys Res 1999;104(D23):30417–26.
[37] Rothman A, Ho T-S, Rabitz H. Observable-preserving control of quantum dynamics over a family of related systems. Phys Rev A 2005;72:023416.
[38] Press WH, Teukolsky SA, Vetterling WT, Flannery BP. Numerical recipes in FORTRAN—The art of science computing. NY: Cambridge University Press; 1992. p. 51.
[39] Qatu MS, Leissa AW. Vibration studies for laminated composite twisted cantilever plates. Int J Mech Sci 1991;33(11):927–40.
[40] Sai Ram KS, Sinha PK. Hygrothermal effects on the free vibration of laminated composite plates. J Sound Vib 1992;158(1):133–48.
[41] Panda HS, Sahu SK, Parhi PK, Asha AV. Vibration of woven fiber composite doubly curved panels with strip delamination in thermal field. J Vib Control 2014. http://dx.doi.org/10.1177/1077546313520024.